PHOTONUCLEAR PRODUCTION OF SELF-TARGETING MEDICAL RADIONUCLIDES USING AN X-BAND ELECTRON LINEAR ACCELERATOR: A FEASIBILITY STUDY

Jaewoong Jang*, Dept. of Bioengineering, University of Tokyo, Bunkyo, Tokyo 113-8656, Japan
Mitsuru Uesaka, Nuclear Professional School, University of Tokyo, Naka, Ibaraki 319-1188, Japan
Masashi Yamamoto, Accuthera Inc., Kawasaki, Kanagawa 215-0033, Japan

Abstract

Motivated by the 2009–2010 global ^{99}Mo/^{99m}Tc supply disruptions, we recently designed an *X*-band electron linear accelerator intended for ^{99}Mo production. Further to this, we examined photonuclear production of radionuclides which can concentrate in body organs without biomolecules. Of particular interest are ^{54}Mn and ^{87m}Sr, which can be produced via ^{55}Mn(γ,n)^{54}Mn and ^{88}Sr(γ,n)^{87m}Sr, respectively. Here we present their radiopharmaceutical potentials, target designs, and expected yields.

INTRODUCTION

Technetium-99m (^{99m}Tc), with which over 80% of all radiopharmaceutical scans are carried out [1], is generally obtained through the negatron (β^-) decay of molybdenum-99 (^{99}Mo). For decades, ^{99}Mo has been supplied as a fission product of ^{235}U [2]. Owing to aging of the involved reactors, however, this fission-based ^{99}Mo supply chain has become fragile, highlighting the need for an alternative ^{99}Mo production method. ^{99}Mo production via the ^{100}Mo photoneutron reaction is an example, for which we recently designed an *X*-band electron linear accelerator (linac) [3, 4]. Thereafter, in an attempt to extend the range of available medical radionuclides, we studied electron-linac-based production of manganese-54 (^{54}Mn) and strontium-87*m* (^{87m}Sr), which we deem potential imaging agents for the heart and bone, respectively.

SELF-TARGETING MEDICAL RADIONUCLIDES

A radiopharmaceutical is essentially a radiolabeled active ingredient (AI) designed to be concentrated in a specific body organ. For instance, when ^{99m}Tc-ECD is administered to a patient, the ECD is taken up by the brain [5], while the ^{99m}Tc provides their location information using its 140.5-keV γ-rays. As such, it is mostly the AI that directs its radiopharmaceutical to the target organ, while the attached radionuclide is used merely for their detection.

Developing an AI requires, however, a substantial research budget and a long period of time. In order to circumvent this research barrier, and to make more radionuclides available for medicine and research, we investigated radionuclides which can concentrate in body organs without AIs and can be produced via photonuclear reactions. ^{54}Mn and ^{87m}Sr are such self-targeting medical radionuclides, of which the decay properties are given in Table 1 [6].

Table 1: Decay Characteristics of ^{54}Mn and ^{87m}Sr

	^{54}Mn	^{87m}Sr
Physical half-life	312.3 d	2.8 h
Emitting radiation	EC[a] γ 834.8 keV (99.9%)	IT[b] γ 388.5 keV (81.9%)
Nuclear reaction	^{55}Mn(γ,n)^{54}Mn	^{88}Sr(γ,n)^{87m}Sr
Target abundance	^{55}Mn: 100%	^{88}Sr: 82.6%
Targeting organ	Myocardium	Bone

[a] Electron capture.
[b] Isomeric transition.

^{54}Mn

We are attempting to produce ^{54}Mn via the ^{55}Mn photoneutron reaction, or ^{55}Mn(γ,n)^{54}Mn; the threshold energy is known to be 10.2 MeV [6].

Studies [7] have shown that the myocardial uptake of ^{54}Mn can be higher than that of ^{201}Tl, a popular heart imaging agent. This stems from the fact that mitochondria, in which manganese is localized, are abundant in the myocardium [7].

As ^{54}Mn exhibits a relatively long physical half-life T_{phy}, it is worth noting that the time during which a radionuclide stays in a body is not simply dictated by T_{phy}, but by the effective half-life T_{eff}:

$$T_{eff} = \frac{T_{phy} T_{bio}}{T_{phy} + T_{bio}}$$

where T_{bio} represents the biological half-life.

Moreover, reasonable production costs are expected from the isotopic abundance of the target material: ^{55}Mn accounts for 100% of naturally occurring manganese (^{nat}Mn).

^{87m}Sr

^{87m}Sr can be produced via ^{88}Sr(γ,n)^{87m}Sr, of which the threshold energy is approximately 11.1 MeV [6].

Belonging to the same group as calcium in the periodic table, strontium has a great affinity to bone matrix [8]. The skeletal system can therefore be visualized by ^{87m}Sr.

Remarkable advantages of ^{87m}Sr are its moderate T_{phy} and γ-ray energy, shown in Table 1. Affordable production costs are also expected, as the natural abundance of ^{88}Sr is as high as 82.6%.

* jang@nuclear.jp

SIMULATION-BASED YIELD ESTIMATION

We performed Monte Carlo (MC) simulations using PHITS version 2.88 [9], for evaluating [4]

$$\mathrm{A}_i(t_{\mathrm{irr}}) = \left[1 - e^{-\lambda_i t_{\mathrm{irr}}}\right] \mathcal{V}_{\mathrm{tar}} I_b \int_{E_{\gamma,\mathrm{min}}}^{E_{\gamma,\mathrm{max}}} \Phi_{\mathrm{MC}}(E_\gamma)\Sigma(E_\gamma)\, dE_\gamma \quad (1)$$

where $\mathrm{A}_i(t_{\mathrm{irr}})$ is the activity of a radionuclide i during target irradiation time t_{irr}, λ_i is the decay constant of i, $\mathcal{V}_{\mathrm{tar}}$ is the target volume, I_b is the electron beam current, E_γ is the bremsstrahlung energy, $\Phi_{\mathrm{MC}}(E_\gamma)$ is the bremsstrahlung fluence obtained by an MC simulation program, and $\Sigma(E_\gamma)$ is the macroscopic cross section for producing i.

The target configurations used in the simulation runs are summarized in Table 2, and illustrated graphically in Fig. 1. Besides, the beam energy and average current of the X-band electron linac we designed, found in Ref. [3], were 35 MeV and 260 μA, respectively. Using these beam parameters, in addition to $\mathcal{V}_{\mathrm{tar}}$ of Table 2 and the photonuclear reaction cross sections contained in TENDL-2009 [10], we evaluated Eq. (1) for ^{54}Mn and ^{87m}Sr.

Table 2: Target Assembly Dimensions

Target	Shape	Parameter (cm)		Volume (cm^3)
$^{\mathrm{nat}}$W	Disk	Radius	2.0	1.26
		Thickness	0.1	
^{55}Mn / ^{88}Sr	Truncated cone	Lower radius	0.5	10.21
		Upper radius	1.5	
		Height	3.0	

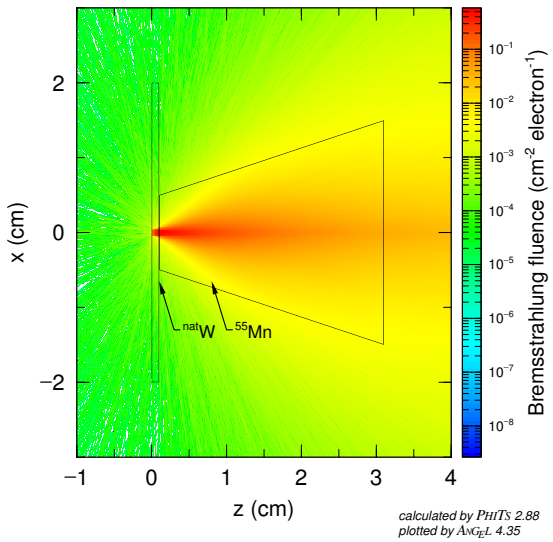

Figure 1: Bremsstrahlung tracks in the $^{\mathrm{nat}}$W-^{55}Mn target assembly simulated at electron beam energy E_e = 35 MeV.

As implied by the exponential term, however, the production rates of the two radionuclides differ to a great extent: the decay constant $\lambda = \frac{\ln 2}{\mathrm{T_{phy}}}$ of ^{87m}Sr is 0.248 h^{-1}, whereas that of ^{54}Mn is as low as 9.248×10^{-5} h^{-1}. Accordingly, rather than plotting their yields with respect to irradiation time, we coplot in Fig. 2 their microscopic cross sections with bremsstrahlung fluences averaged over the respective target volumes, and tabulate their activities in Table 3. Here t_{irr} for ^{88}Sr(γ,n)^{87m}Sr was selected considering the time at which the ^{87m}Sr activity converges to its maximal activity, which is approximately 7T$_{\mathrm{phy}}$:

$$1 - e^{-\frac{\ln 2}{\mathrm{T_{phy}}}(7\mathrm{T_{phy}})} \approx 0.992$$

On the other hand, because 7T$_{\mathrm{phy}}$ of ^{54}Mn is impractically long for target irradiation, t_{irr} for ^{55}Mn(γ,n)^{54}Mn was chosen taking into account the time during which the natural tungsten ($^{\mathrm{nat}}$W) bremsstrahlung converter can withstand the thermal stress.

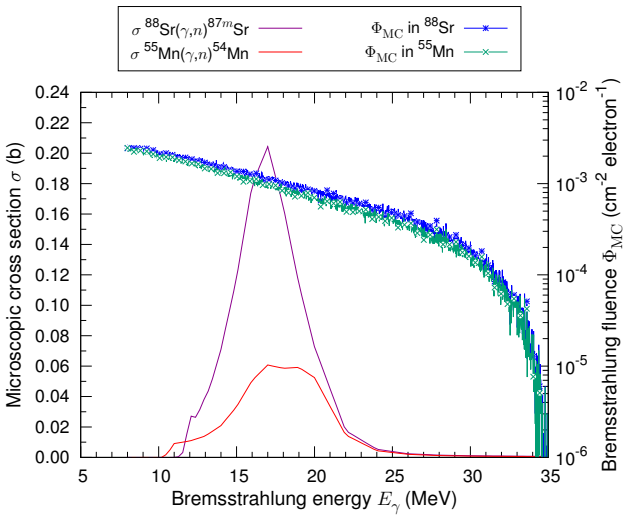

Figure 2: Microscopic cross sections contained in TENDL-2009 and volume-averaged bremsstrahlung fluences calculated at E_e = 35 MeV.

Table 3: Evaluation Results of Eq. (1)

Product	t_{irr} to saturation activity (~ 7T$_{\mathrm{phy}}$)	t_{irr}	A$_i(t_{\mathrm{irr}})$
^{54}Mn	2186.1 d	72 h	170.8 GBq
^{87m}Sr	19.6 h	18 h	14.5 TBq

Although the evaluated ^{54}Mn and ^{87m}Sr activities are the ones before chemical processing and delivery to end users, considering the activity loss factors of ^{99}Mo/^{99m}Tc supply chain and average dose of commercial radiopharmaceuticals, we find the resulting ^{54}Mn and ^{87m}Sr activities fairly high. Utilizing the compactness of the designed X-band electron linac, then, sufficient quantities of these self-targeting radionuclides can be supplied with satisfactory accessibility.

POST-IRRADIATION CHEMICAL PROCESSING

Following its production, a medical radionuclide should be chemically processed to meet pharmacopeial standards. Examples include pH adjustment and additive addition, and chemical separation if the radionuclide in question is obtained through its parent. Furthermore, as mentioned earlier, almost all medical radionuclides are compounded with organic molecules to form radiopharmaceuticals. In contrast, as ^{54}Mn and ^{87m}Sr are designed to be self-targeting, and can be produced directly from photonuclear reactions, simpler chemical processing is expected.

SUMMARY

Conventional radiopharmaceuticals are a mixture of biomolecules and radionuclides, the former of which make radiopharmaceutical development demanding. In a bid to bypass this involvement of biomolecules or AIs, and to extend the range of electron-linac-producible medical radionuclides, we examined the radiopharmaceutical potentials, photonuclear production methods, and yields of ^{54}Mn and ^{87m}Sr. We expect that using the X-band electron linac we recently designed can enable producing these self-targeting medical radionuclides in close proximity to radiopharmacies or laboratories.

REFERENCES

[1] OECD Nuclear Energy Agency, "The supply of medical radioisotopes: 2017 medical isotope supply review: ^{99}Mo/^{99m}Tc market demand and production capacity projection 2017-2022", OECD, Paris, France, Rep. HLGMR2017-2, Apr. 2017.

[2] National Academies of Sciences, Engineering, and Medicine, *Molybdenum-99 for medical imaging*. WA, USA: National Academies Press, 2016.

[3] J. Jang, M. Yamamoto, and M. Uesaka, "Development of a compact X-band electron linac for production of Mo-99/Tc-99m", in *Proc. 7th Int. Particle Accelerator Conf. (IPAC'16)*, Busan, Korea, May 2016, paper TUPOY007, pp. 1917–1920.

[4] J. Jang, M. Yamamoto, and M. Uesaka, "Design of a compact X-band electron linear accelerator dedicated to decentralized production of ^{99}Mo/^{99m}Tc", submitted for publication.

[5] S. R. Cherry, J. A. Sorenson, and M. E. Phelps, *Physics in Nuclear Medicine*, 4th ed. Philadelphia, PA, USA: Saunders, 2012.

[6] S. Y. F. Chu, L. P. Ekström, and R. B. Firestone; `http://nucleardata.nuclear.lu.se/toi/`

[7] D. M. Chauncey, Jr. *et al.*, "Tissue distribution studies with radioactive manganese: a potential agent for myocardial imaging", *J. Nucl. Med.*, vol. 18, no. 9, pp. 933–936, Sept. 1977.

[8] S. G. Dahl *et al.*, "Incorporation and distribution of strontium in bone", *Bone*, vol. 28, no. 4, pp. 446–453, Apr. 2001.

[9] T. Sato *et al.*, "Particle and Heavy Ion Transport code System, PHITS, version 2.52", *J. Nucl. Sci. Technol.*, vol. 50, no. 9, pp. 913–923, Sept. 2013.

[10] A J. Koning and D. Rochman, "Modern nuclear data evaluation with the TALYS code system", *Nucl. Data Sheets*, vol. 113, no. 12, pp. 2841–2934, Dec. 2012.